Approximations to the Wave Propagation Transfer Function

Philip Schultz

In homogeneous media, propagation of a wave disturbance can be expressed in terms of a linear spatial filter. To see this let us consider a monochromatic wave disturbance, $p(x,z,\omega)$, in two dimensions and write

$$p(x,z,\omega) = \int_{-\infty}^{\infty} P(k_x,z,\omega) \, e^{ik_x x} \, dk_x \, , \tag{1}$$

where equation (1) expresses the Fourier transform over the horizontal coordinate. Now we wish to find a relation between $P(k_x,z,\omega)$ and $P_0(k_x,0,\omega)$, so we use equation (1) in the monochromatic wave (Helmholtz) equation,

$$(\partial_{xx} + \partial_{zz}) \, p(x,z,\omega) = \frac{\omega^2}{c^2} \, p(x,z,\omega) \, . \tag{2}$$

This reduces to

$$\frac{d^2}{dz^2} P(k_x,z,\omega) + (\frac{\omega^2}{c^2} - k_x^2) \, P(k_x,z,\omega) = 0 \tag{3}$$

Equation (3) is a familiar one-dimensional ordinary differential equation, a solution to which we can write immediately as

$$P(k_x,z,\omega) = P_0(k_x,0,\omega) \, e^{i\sqrt{\frac{\omega^2}{c^2} - k_x^2} \, z} \, . \tag{4}$$

Equation (4) expresses the desired result where we identify

$$e^{i\sqrt{\frac{\omega^2}{c^2} - k_x^2} \, z} \tag{5}$$

with a transfer function in the x-transform domain. Since this operation becomes a convolution in the x domain, we can identify the transform of expression (5) with the response of a point aperture in the x-dimension to an incident monochromatic wave.

We graphically show expression (5), which is an exact solution, for purposes of comparing later with approximations. Figures 1 show this function numerically transformed over various parameters.

The first approximation considered here is a binomial approximation to the square root operator for small k_x . We have

$$\exp\left[i\sqrt{\frac{\omega^2}{c^2} - k_x^2}\, z \right] \cong \exp\left[i \frac{\omega}{c}\left(1 - \frac{k_x^2 c^2}{2\omega^2} \right) z \right] \qquad (6)$$

Notice that expression (6), unlike (5), maintains a propagation-like solution for $k_x^2 > \frac{\omega^2}{c^2}$. Clearly, one would like $k_x^2 > \frac{\omega^2}{c^2}$ to give evanescent behavior, so it is found to be advantageous to truncate to zero the expression (6) for $k_x^2 > \frac{\omega^2}{c^2}$.

An interesting feature of this approximation is that its rational form allows an exact Fourier transform to be done. Although transforms can easily be done over both k_x and ω , shown below is the transform over k_x only.

$$\text{F.T.}_{k_x}\left[e^{\, i \frac{\omega}{c}\left(1 - \frac{k_x^2 c^2}{2\omega^2} \right) z} \right] = \sqrt{\frac{2\pi\omega}{cz}}\, e^{\, i\left(\frac{\omega}{c} z + \frac{\omega x^2}{2cz} - \frac{\pi}{4} \right)} \qquad (7)$$

Equation (7) represents the response in the x-z plane for a monochromatic wave impinging on a point aperture in the x-dimension. To look at the geometric form that lines of constant phase take, we let

$$\frac{\omega}{c} z + \frac{\omega x^2}{2cz} - \frac{\pi}{4} = \text{constant} \cong \frac{2\omega}{c} z_o - \frac{\pi}{4}$$

which reduces to

$$\frac{(z-z_o)^2}{z_o^2} + \frac{x^2}{2z_o^2} = 1 \tag{8}$$

Equation (8) gives an ellipse in the x-z plane for constant ω. In other words, one of the effects of the approximation is to replace circular wavefronts with elliptical ones. This is the same wavefront distortion that is caused by the Fresnel approximation. In the Fresnel approximation, the distance $r = \sqrt{x^2+z^2}$ is approximated by

$$z\left(1 + \frac{x^2}{2z^2}\right) \cong r = ct$$

which, for constant time, gives elliptical wavefronts with similar geometries.

Expression (6) and various Fourier transformations can be seen in figures 2.

The last approximation is given by

$$\exp\left[i\sqrt{\frac{\omega^2}{c^2} - k_x^2}\; z\right] \cong \exp\left[i \frac{\omega}{c} \frac{\left(1-\frac{3}{4}\frac{k^2c^2}{\omega^2}\right)}{\left(1-\frac{1}{4}\frac{k^2c^2}{\omega^2}\right)} z\right] \tag{9}$$

Equation (9) suffers similar problems of non-evanescent behavior at $k_x^2 > \frac{\omega^2}{c^2}$, so truncation again is imposed. This expression and its Fourier transforms are depicted in figures 3.

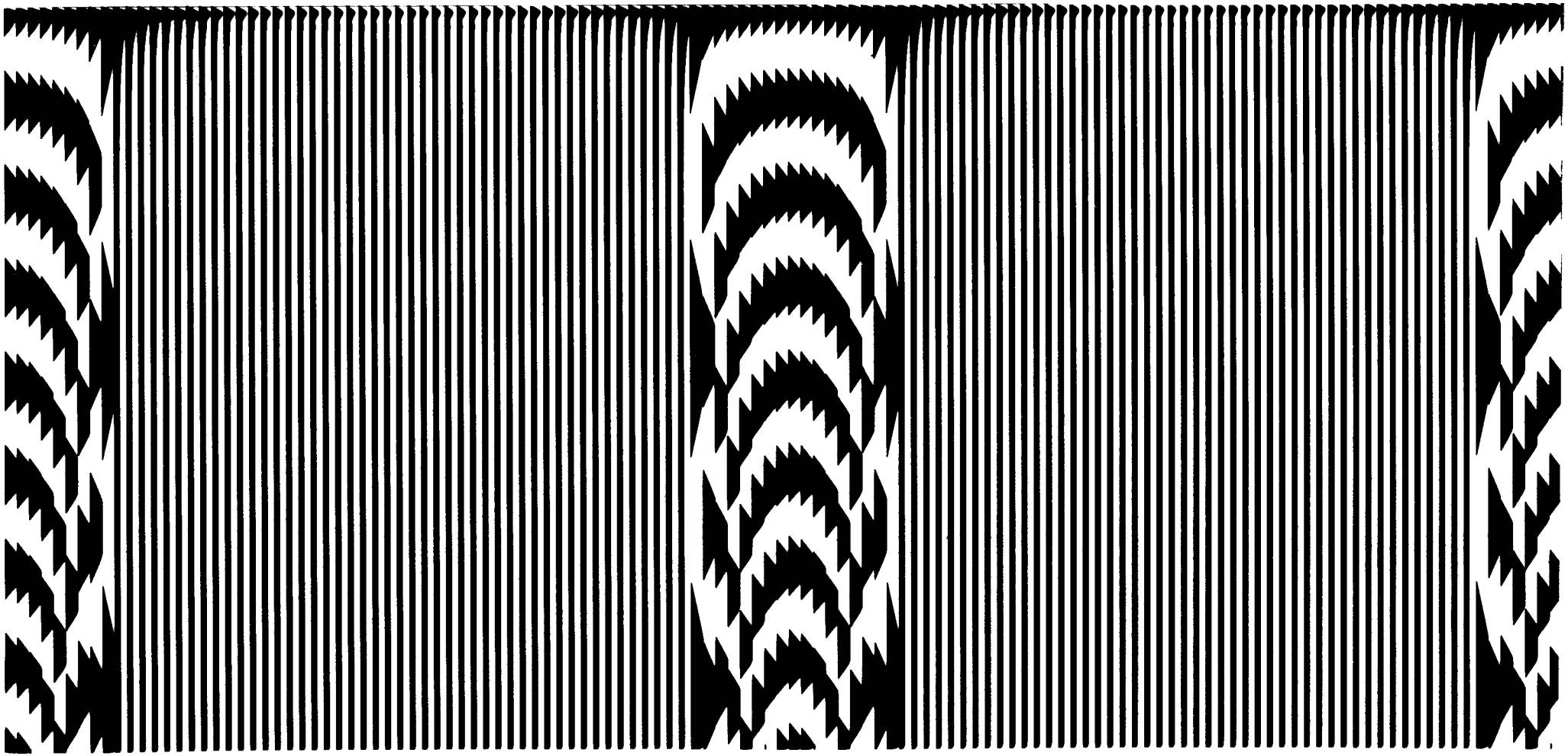

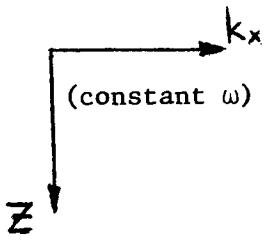

Figure 1a:

The exact transfer function, $\exp[\, i\sqrt{\frac{\omega^2}{c^2} - k_x^2}\; z\,]$, plotted k_x versus z with ω taken as constant. The abrupt change in character of the function occurs at $\frac{\omega^2}{c^2} = k_x^2$, the transition between propagation and evanescence.

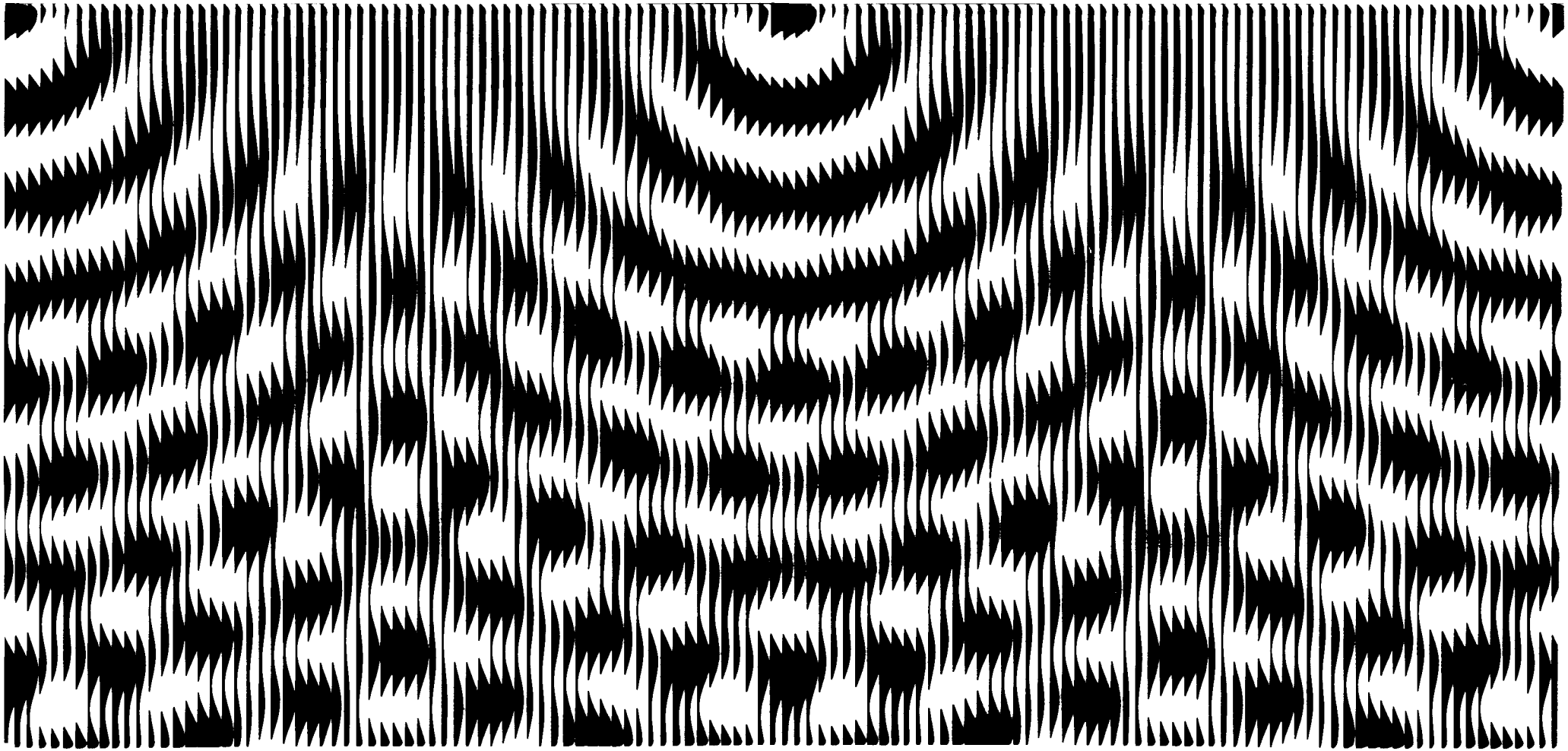

Figure 1b:

The exact transfer function, Fourier transformed over k_x, and plotted x versus z with constant ω. This may be interpreted physically as repetitive periodic responses of point apertures in the x-dimension to an incident monochromatic plane wave. The repetition of sources is due to the periodic boundary conditions inherent in the fast Fourier transform (FFT). Since no approximations have been made, the wavefronts are perfectly circular.

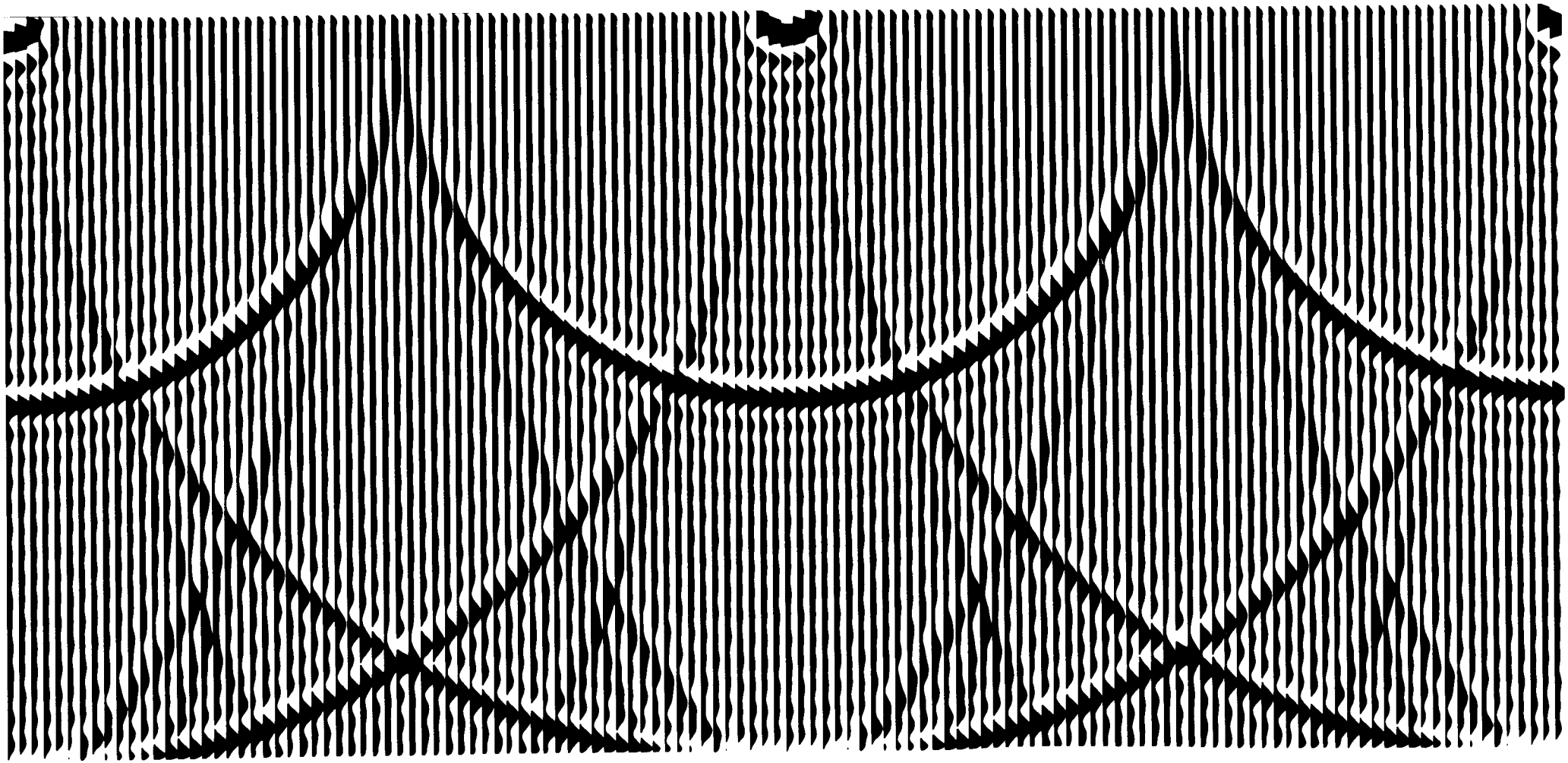

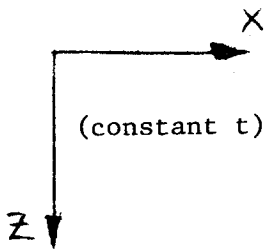

Figure 1c:

A simulation of the transformation of the exact transfer function over k_x and ω. The transform over k_x was done exactly (using FFT). However, the transform over ω was simulated by a summation over 15 frequencies (rather than an infinite number) to reduce expense. The plot is x versus z at constant time, and should show a circular delta-function wavefront representing an impulsive incident wave at the aperture. The repetition of the pulse in time is due to the artificial Fourier transformation over ω. Four wavefronts are visible radiating from the sources at the corners.

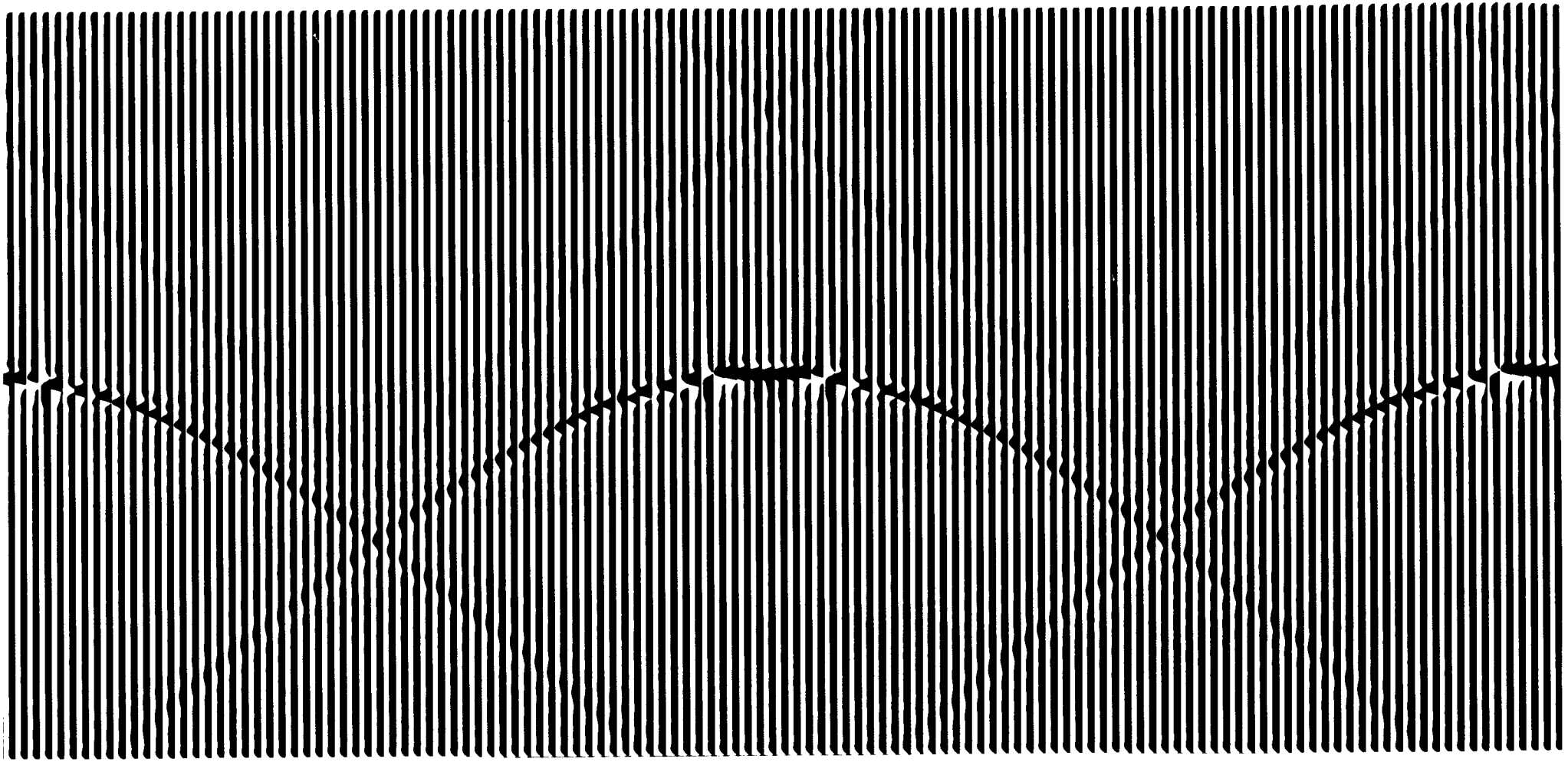

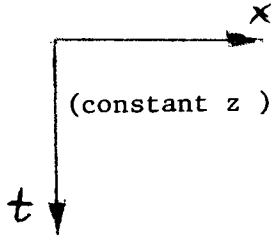

Figure 1d:

The exact transfer function transformed over k_x and ω for constant z. This transformation, unlike that of figure 1c, did not have to be simulated. The figure shows x versus t for constant z and is the familiar hyperbola of a point scatterer. The scale is one to one (i.e., the asymptotes are at 45°). Notice the ghost-like lines in the upper 1/2 of the figure. These are the continuation of the tails of the hyperbolas below due to repetition now in both linear dimensions. The rather confused waveform at the apeces are a result of the difficulty in representing a delta-function on a grid.

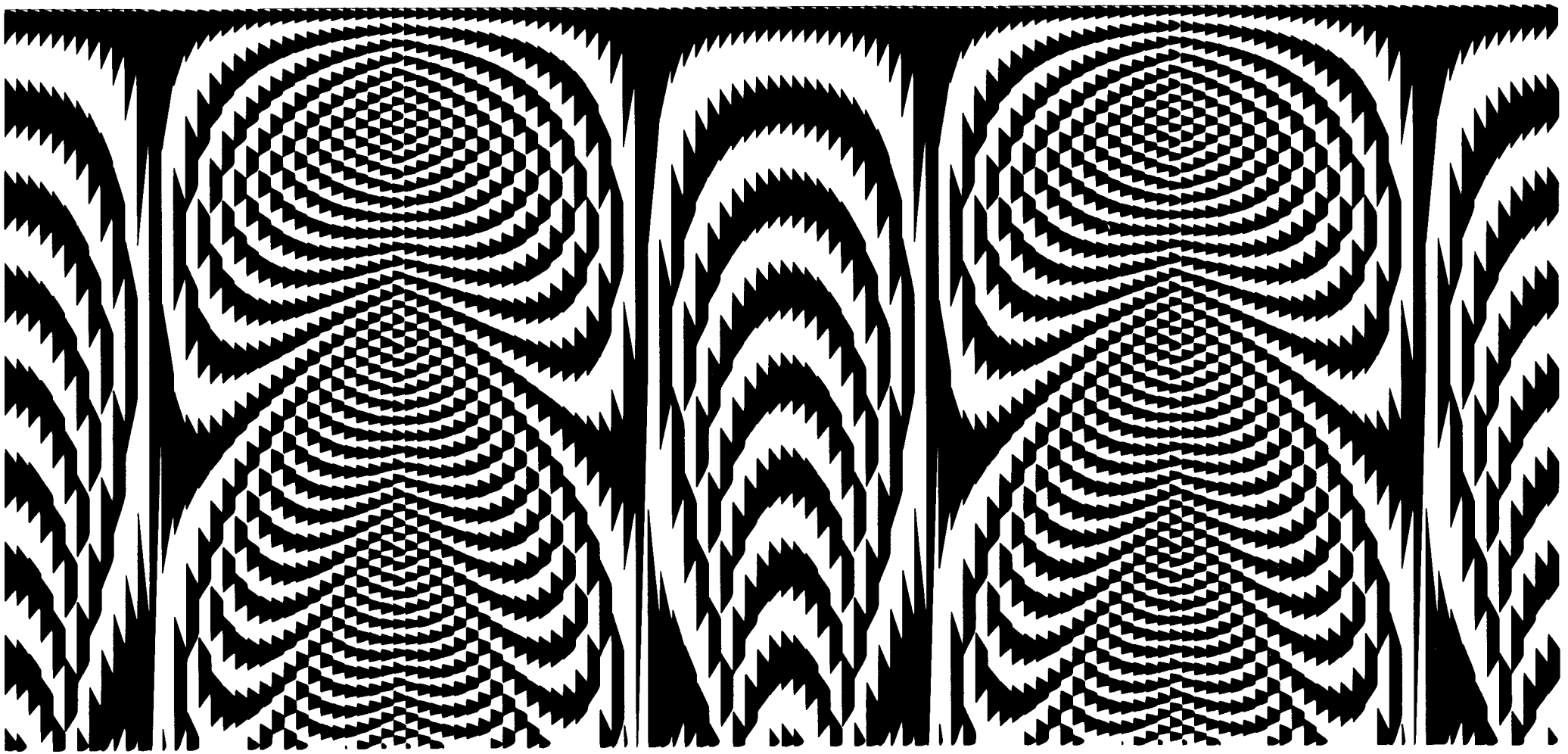

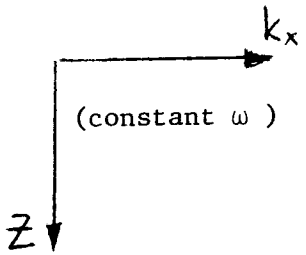

Figure 2a:
The parabolic transfer function, $\exp[\, i \frac{\omega}{c} \left(1 - \frac{k_x^2 c^2}{2\omega^2} \right) z \,]$, plotted k_x versus z with constant ω. The interesting pattern is due to the approximation maintaining a propagating character when $k_x^2 > \frac{\omega^2}{c^2}$, rather than becoming evanescent.

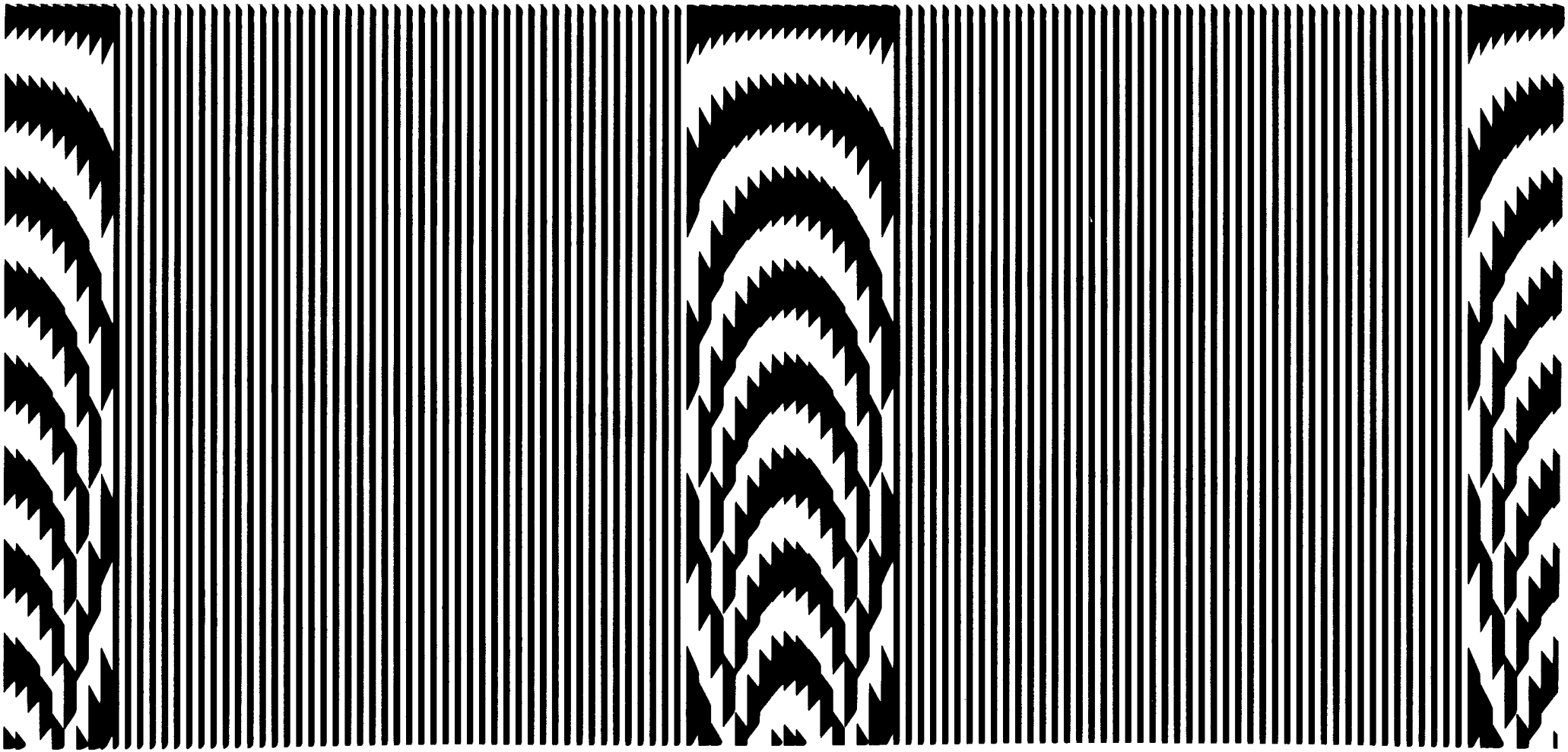

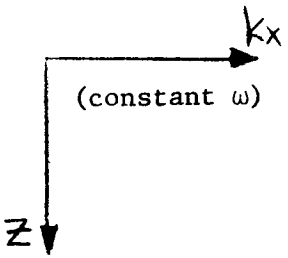

Figure 2b:

This the parabolic transfer function and is the same as figure 2a but truncated to zero for $k_x^2 > \frac{\omega^2}{c^2}$ to simulate proper evanescent behavior.

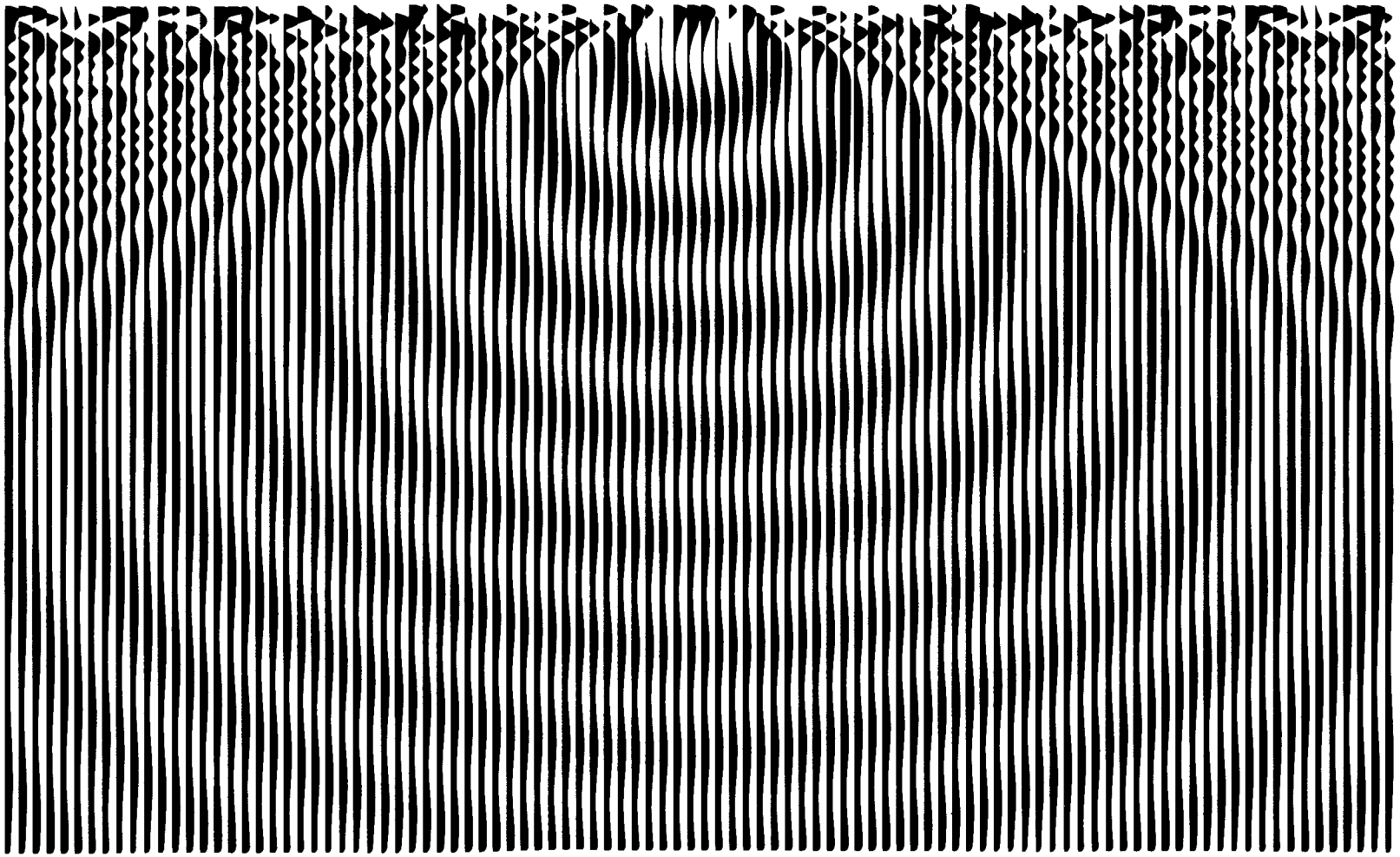

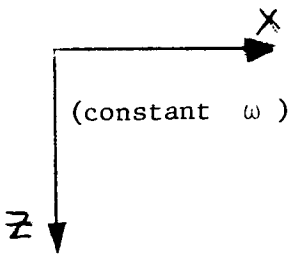

Figure 2c:

The parabolic transfer function Fourier transformed over k_x and plotted x versus z with ω constant. The transformation was obtained exactly through analytical techniques (see text). The function transformed is shown in figure 2a, i.e., the propagating character was maintained throughout the domain of k_x. One can clearly see the elliptical wavefronts derived in the text.

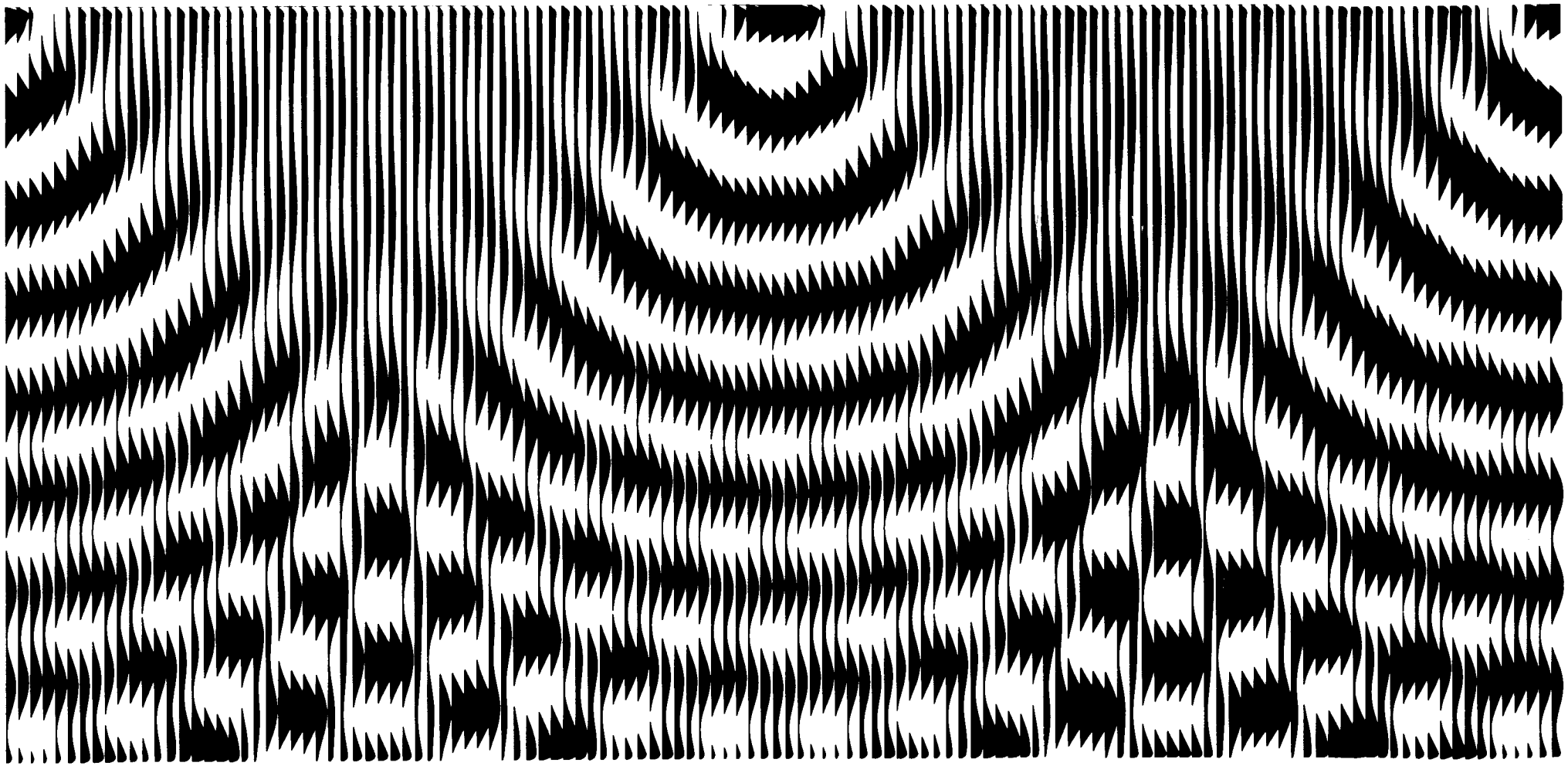

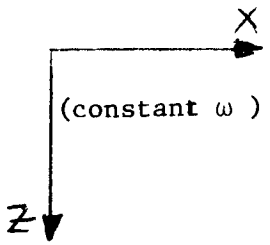

Figure 2d:

The truncated parabolic transfer function (shown in figure 2b) fast Fourier transformed over k_x to show x versus z for constant ω . Compare with the exact form, figure 1b.

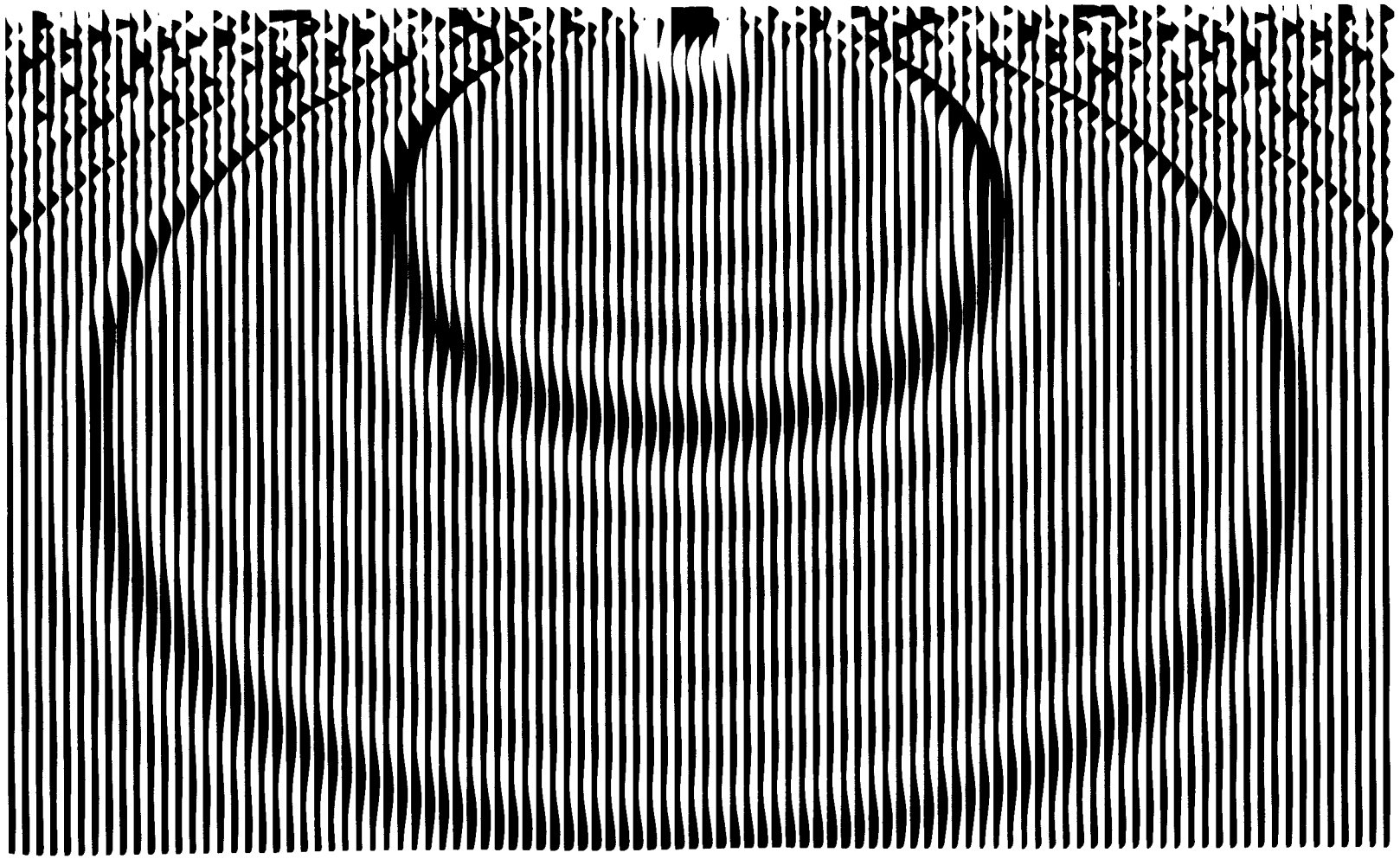

Figure 2e:

A simulation over ω of the Fourier transform of the non-truncated (figure 2a) parabolic transfer function. Shown is x versus z for constant time. The simulation was obtained by summation over 5 frequencies, and attempts to show the response of the point aperture to an incident delta-function wavefront. Careful examination will show that this wavefront gives a good approximation to circular wavefronts when restricted to within 15° of the vertical.

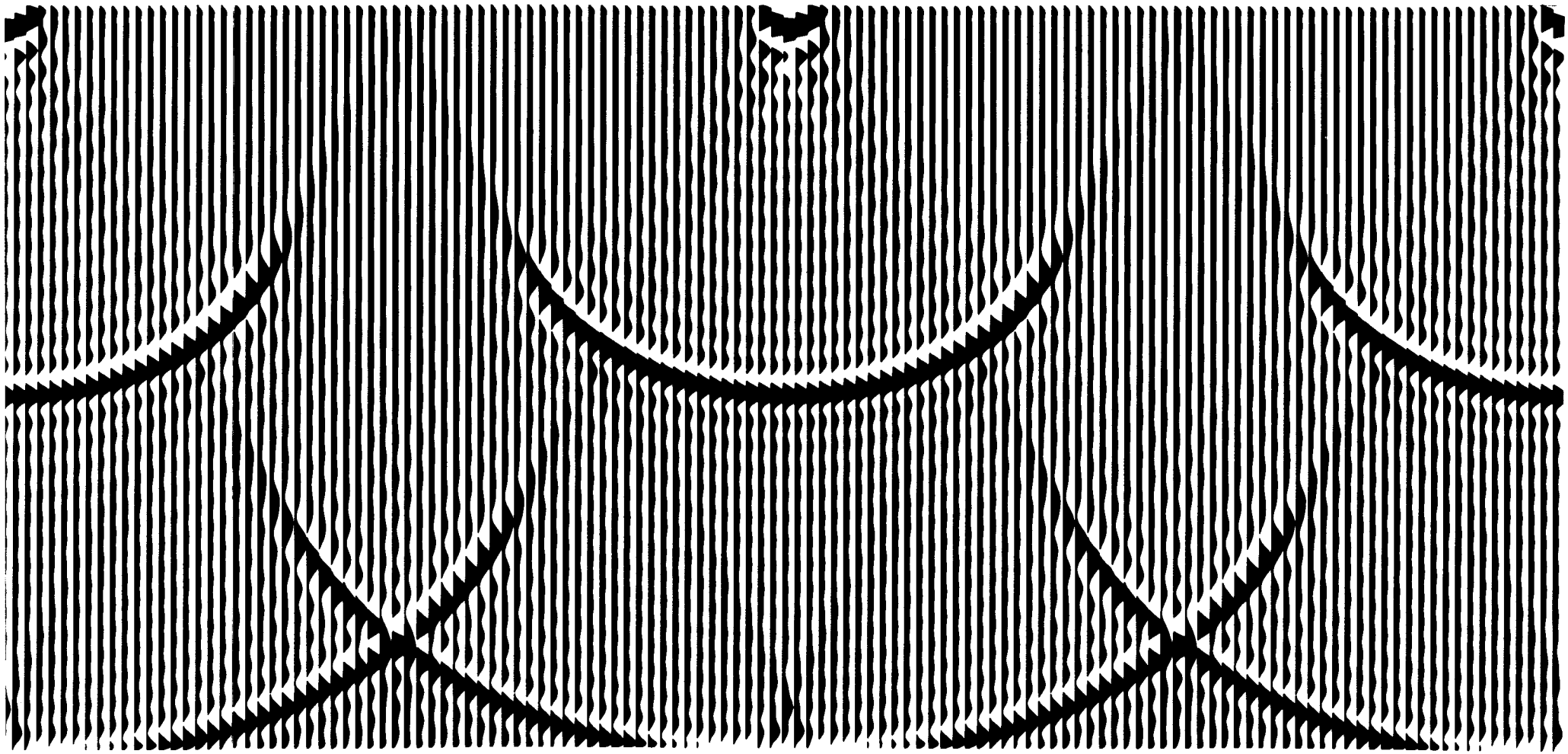

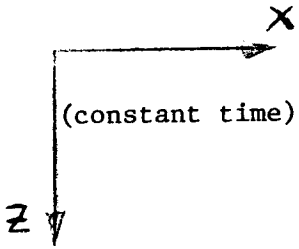

Figure 2f:

A simulation of the Fourier transformation over ω of the truncated parabolic transfer function (figure 2b). Shown is x versus z for constant time. 15 frequencies were summed to enter the time domain, and periodic wavefronts in time can be seen. Notice that the forced evanescence, as opposed to non-truncated form depicted in figure 2e, causes amplitude attenuation with increasing angle from the vertical. Compare with exact form shown in figure 1c.

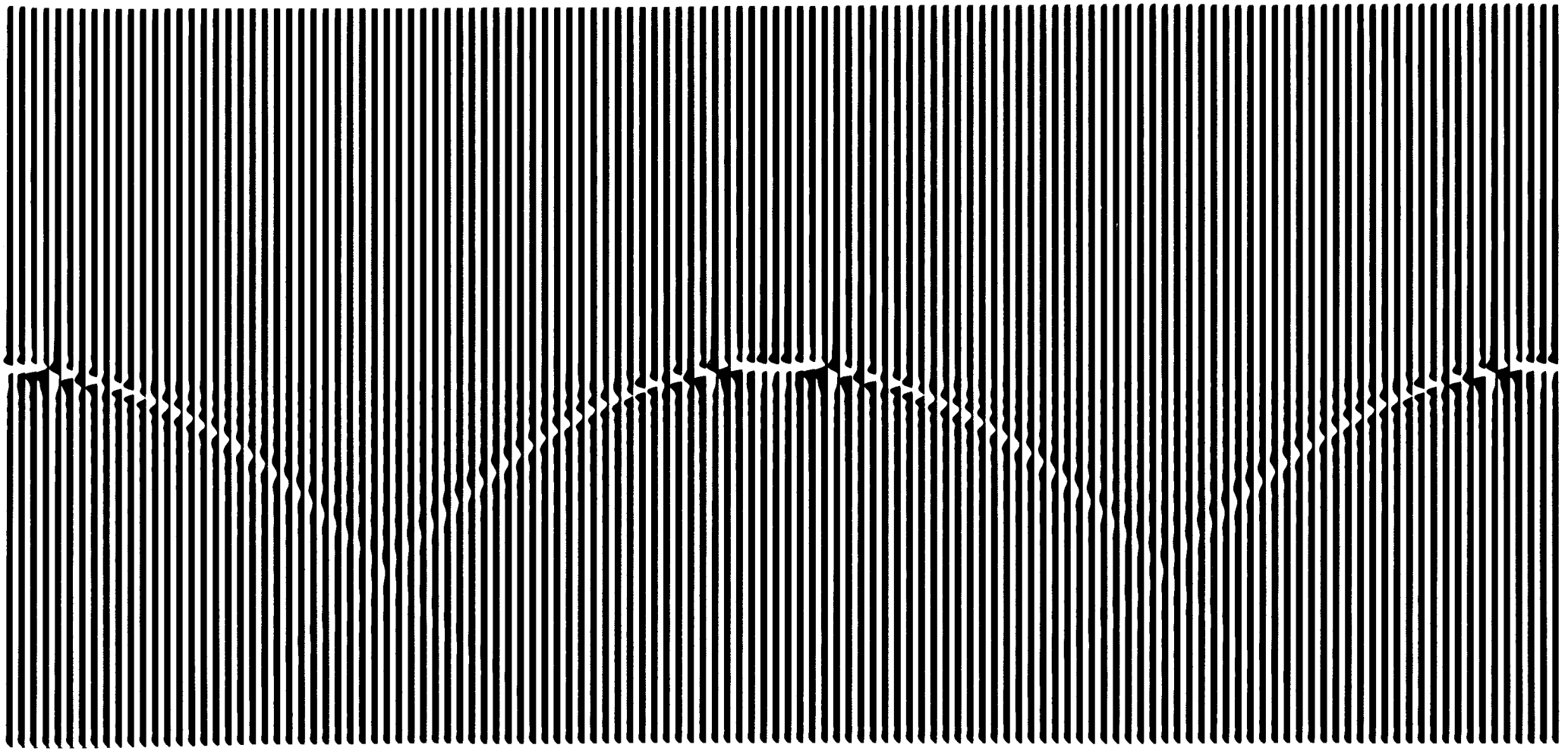

Figure 2g:

The truncated parabolic transfer function transformed over k_x and ω for constant z. As in figure 1d (with which this figure should be compared) the scale is one to one. The tails fade out rather quickly, and it is not obvious from the figure, but can be shown mathematically, that the asymptotes are vertical, i.e., the geometric form is that of a parabola.

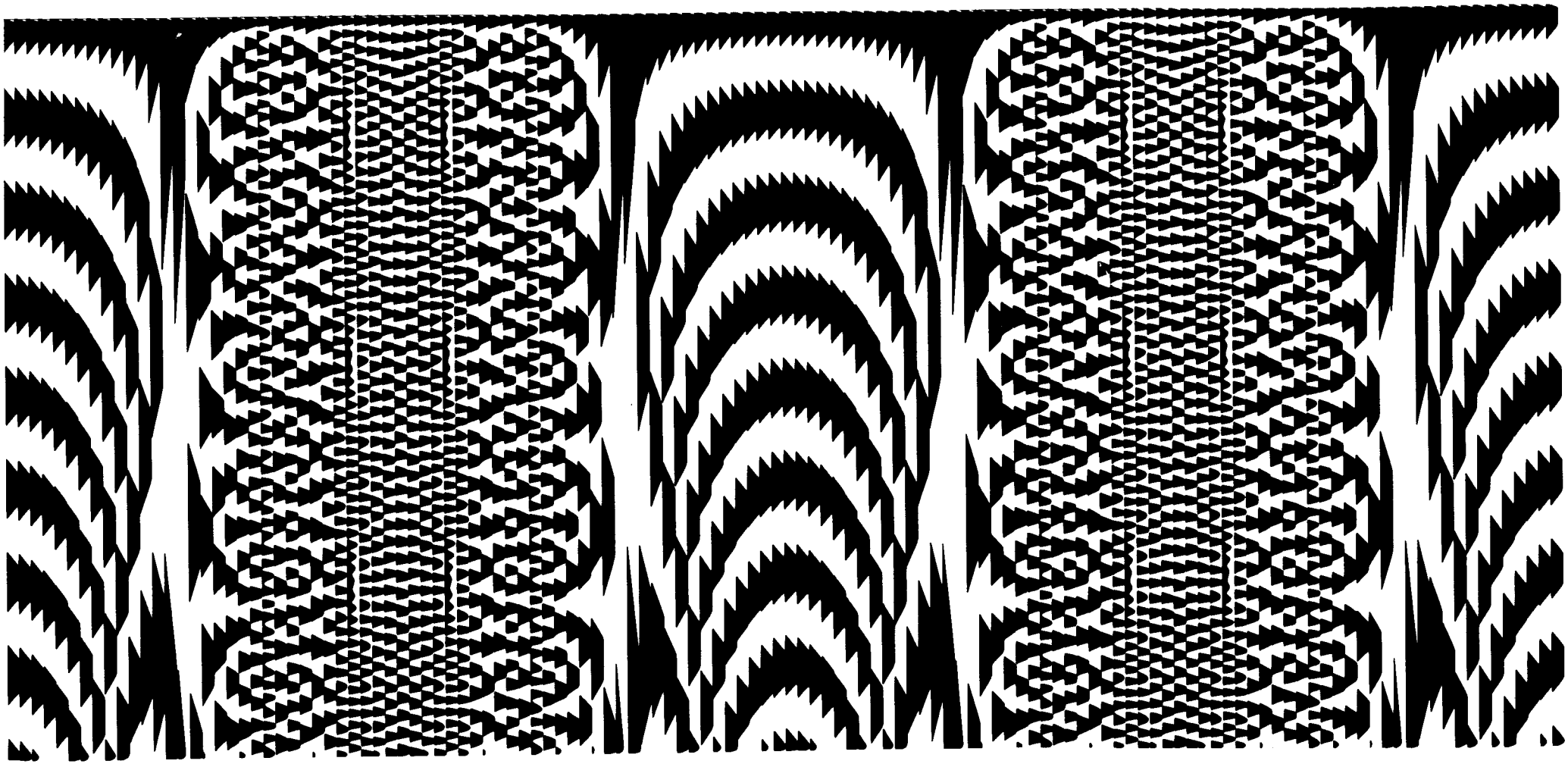

Figure 3a:

The non-truncated 45° transfer function, $\exp\left[i \frac{\omega}{c} \frac{(1- \frac{3}{4} \frac{k_x^2 c^2}{\omega^2})}{(1 - \frac{1}{4} \frac{k_x^2 c^2}{\omega^2})} z \right]$, plotted k_x versus z with ω constant. The interesting pattern is again due to the approximation maintaining a propagating character when $k_x^2 > \frac{\omega^2}{c^2}$, rather than becoming evanescent.

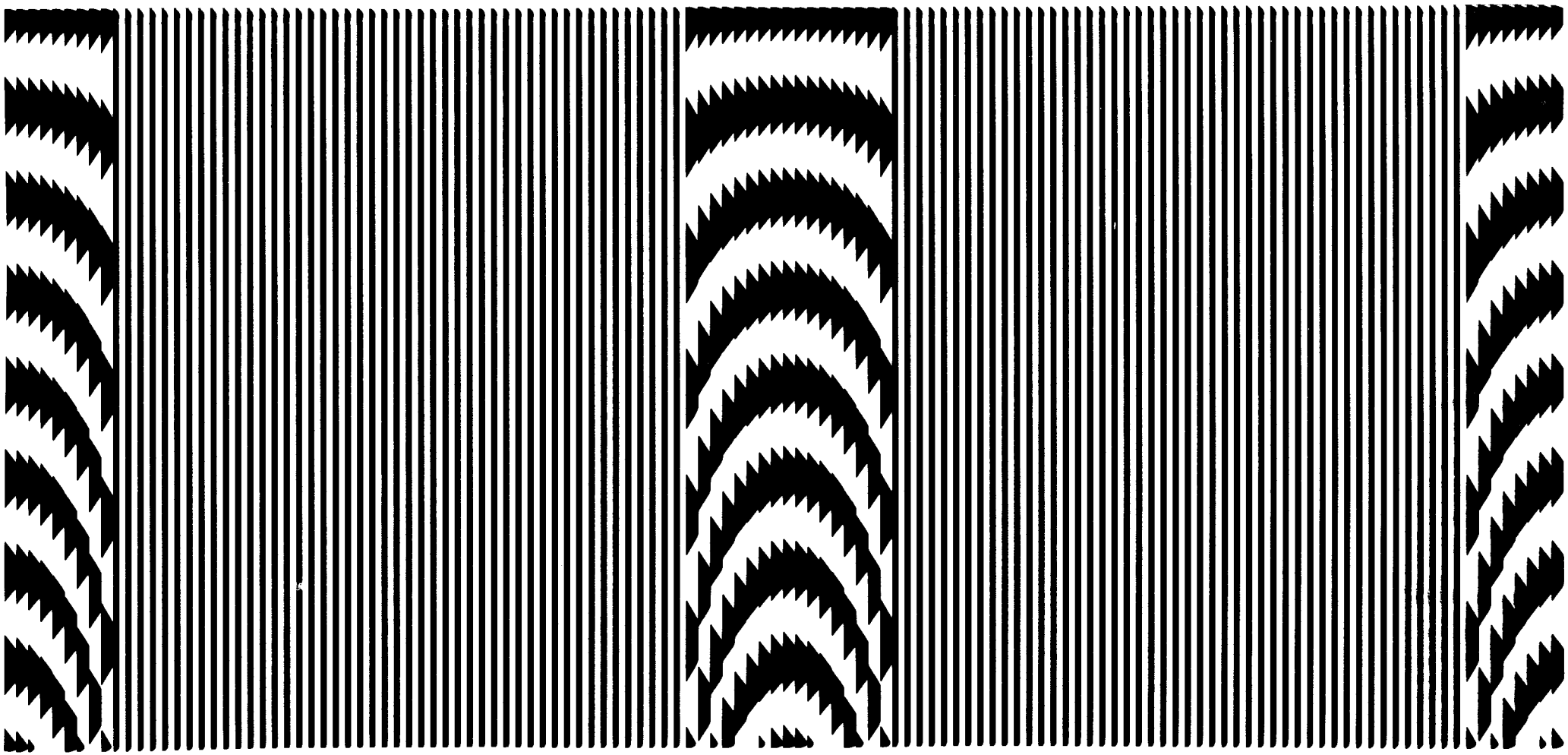

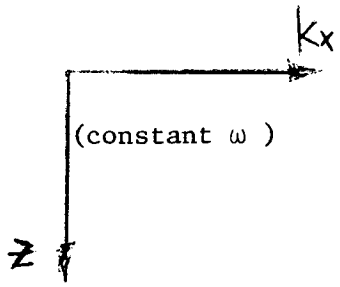

Figure 3b:

This is the 45° transfer function and is the same as figure 3a but truncated to zero for $k_x^2 > \frac{\omega^2}{c^2}$ to simulate proper evanescent behavior.

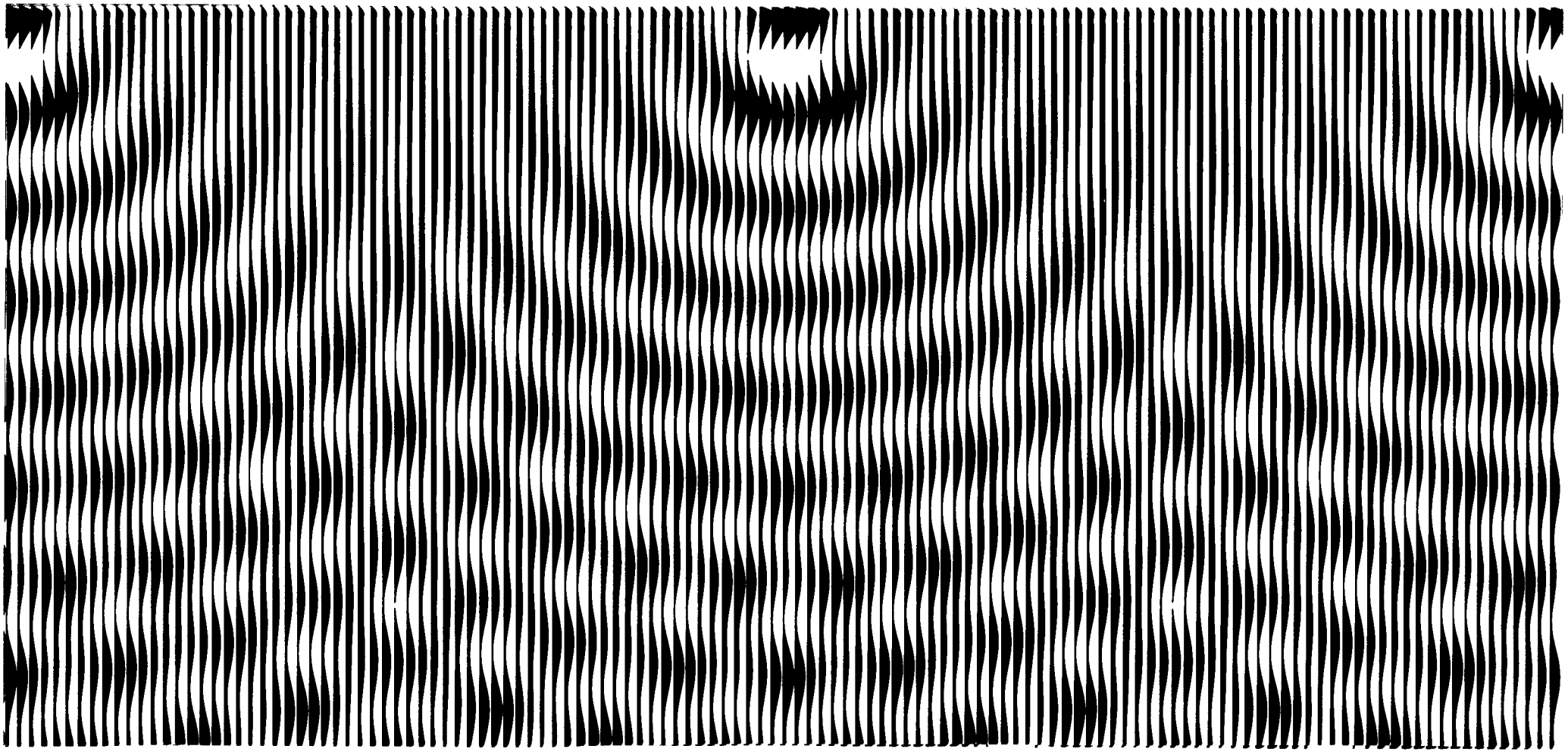

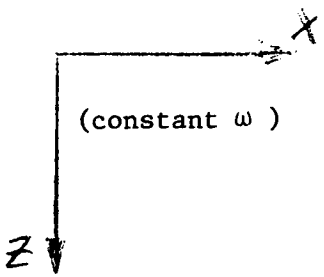

Figure 3c:

The truncated 45° transfer function (shown in figure 3b) fast Fourier transformed over k_x to show x versus z for constant ω . Compare with exact form, figure 1b.

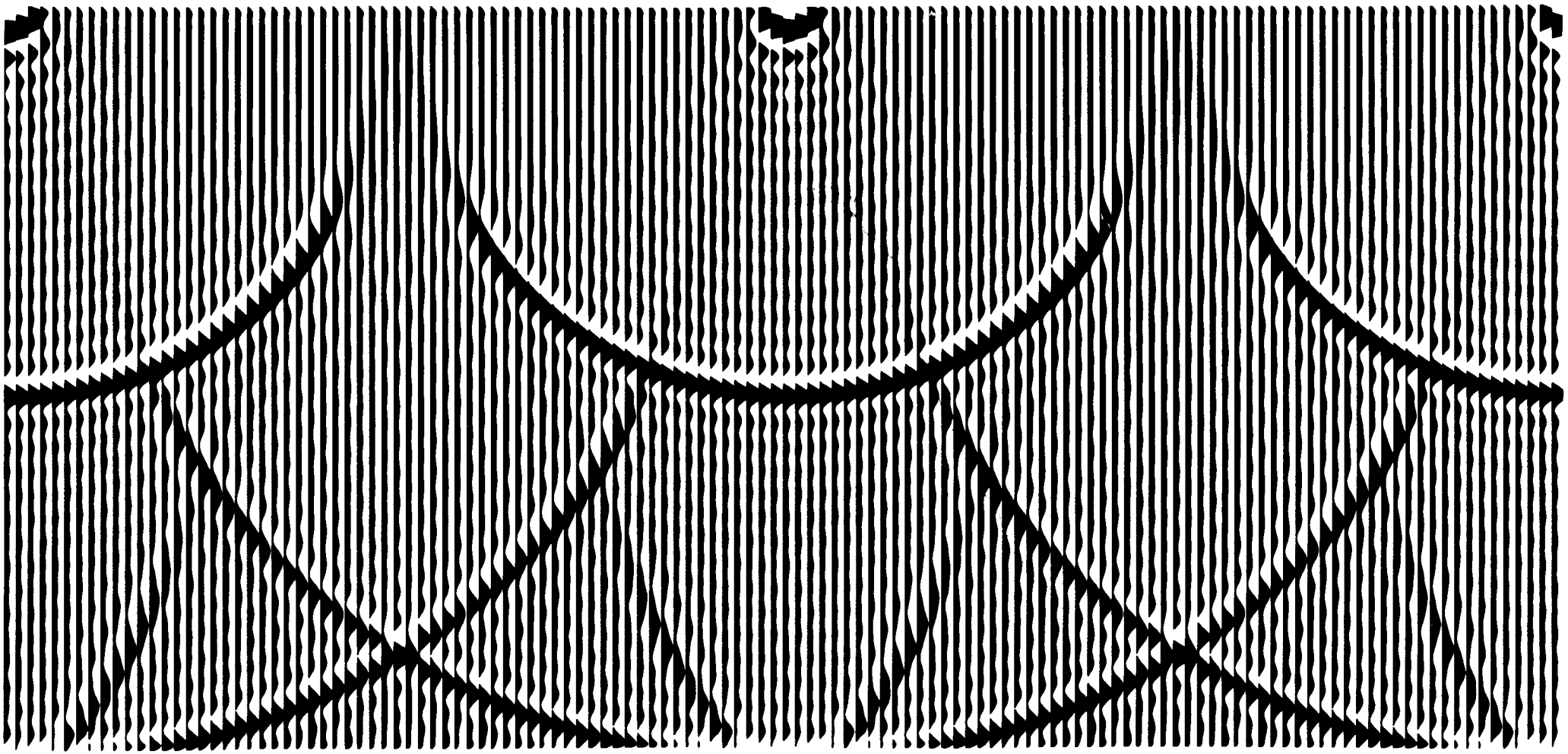

Figure 3d:

A simulation of the Fourier transformation over ω of the truncated 45° transfer function (figure 3b). Shown is x versus z for constant time. Fifteen frequencies were summed to enter the time domain, and periodic wavefronts in time can be seen. Compare with the exact form shown in figure 1c.

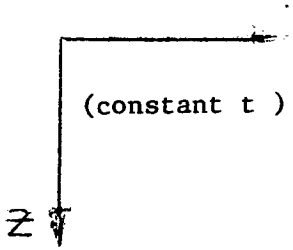

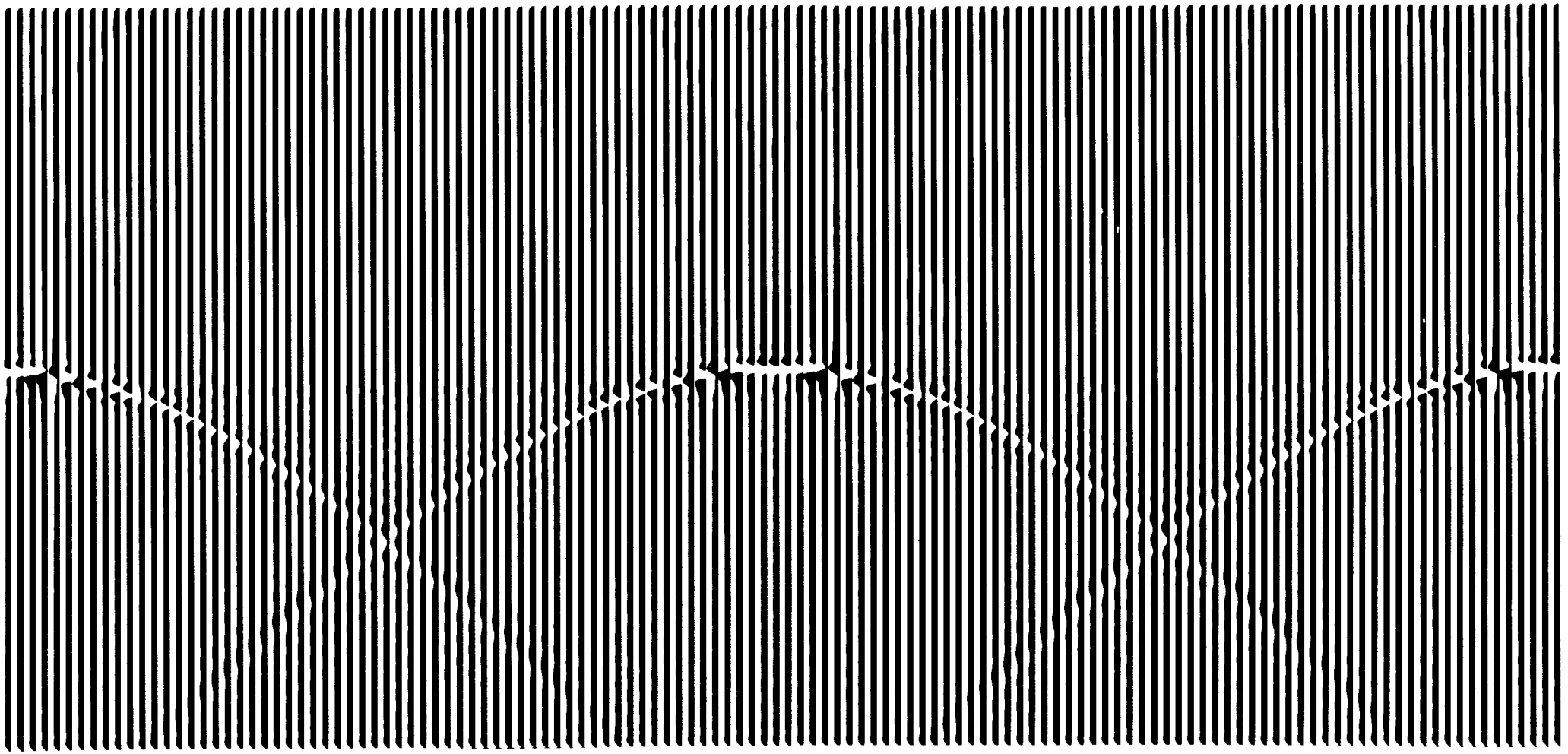

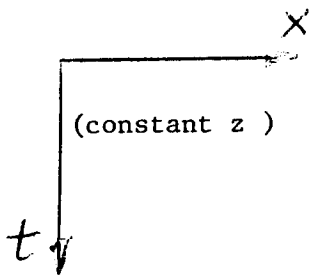

Figure 3e:

The truncated 45° transfer function transformed over k_x and ω for constant z. As in figure 1d (with which this figure should be compared)the scale is one to one. Notice that the tails fade out more rapidly than in the exact case, but less rapidly than in the parabolic case.